

Resonance Hopping Transfers Between Moon Science Orbits



AE8900 MS Special Problems Report
Space Systems Design Laboratory (SSDL)
Guggenheim School of Aerospace Engineering
Georgia Institute of Technology
Atlanta, GA

Author:
Adam T. Brinckerhoff

Advisor:
Dr. Ryan P. Russell

April 22, 2009

Resonance Hopping Transfers Between Moon Science Orbits

Adam T. Brinckerhoff*

Georgia Institute of Technology, Atlanta, GA, 30332-0150

Resonance hopping transfers between science orbits around two circular, coplanar moons of a common planet are designed using series of alternating V-infinity leveraging maneuvers and zero-point patched conic gravity assists. When this technique is combined with an efficient global search based on Bellman's Principle, the end result is an exhaustive set of fuel and time optimal trajectories between the two moons in question. The associated Pareto front of solutions represents the classic fuel versus flight time trade study sought in preliminary mission design. Example numerical results are produced for orbital transfers between scientifically interesting moons in the Jovian system due to NASA and ESA's particular interest in executing future tour missions in this environment. Finally, resonant transfers between neighboring pairs of moons are patched together to obtain fuel and flight time estimates for a full Jovian system tour between intermediate previously discovered circulating eccentric science orbits. Results from this fast, preliminary design procedure are intended to serve as useful starting points for higher fidelity multi-body mission design. In general, the resonant hopping design approach and the associated design procedure are found to be most relevant for missions with short flight time requirements.

Nomenclature

V_{∞}	= Excess Hyperbolic Velocity	\mathbf{V}_M	= Planet-relative Moon Velocity Vector
VILM	= V_{∞} Leveraging Maneuver	$\mathbf{V}_{\infty IN}$	= Excess Hyperbolic Spacecraft Approach Velocity Vector
L	= Number of Spacecraft Orbit Revolutions	$\mathbf{V}_{\infty OUT}$	= Excess Hyperbolic Spacecraft Departure Velocity Vector
K	= Number of Moon Orbit Revolutions	θ	= Initial Transfer Moon Phase Angle
R_p	= Ratio Between Spacecraft and Resonant Orbit Periods	rp_{nec}	= Necessary Radius of Closest Approach for Flyby
M	= Spacecraft Orbit Revolution on which the Maneuver is Performed	rp_{min}	= Minimum Radius of Closest Approach for Flyby
\pm	= Rendezvous After or Before the Line of Apesides Crossing	μ_m	= Moon Gravitational Parameter
Δv_{ESC}	= Magnitude of Escape Propulsive Maneuver at Moon	k_{nec}	= Necessary Turn Angle of the V_{∞} Vector for Flyby
Δv_{SPM}	= Magnitude of Small Propulsive Maneuver at Line of Apesides	HT	= Hohmann Transfer
\mathbf{V}_{IN}	= Planet-relative Spacecraft Approach Velocity Vector	FOT	= Fuel Optimum Trajectory
\mathbf{V}_{OUT}	= Planet-relative Spacecraft Departure Velocity Vector	TOT	= Time Optimum Trajectory

* Graduate Research Assistant, Daniel Guggenheim School of Aerospace Engineering, Georgia Institute of Technology, 270 Ferst Drive, Atlanta, GA 30332-0150.

I. Introduction

A V_∞ leveraging maneuver (VILM) is defined as a technique that utilizes a propulsive burn well before arriving at a gravity assist body in order to efficiently increase or decrease the arrival V_∞ (excess hyperbolic velocity). At the expense of extra flight time, the typical effect of the propulsive ΔV maneuver and associated flyby is a significant amplification in the change in V_∞ (that otherwise would be directly changed using a launch vehicle or propulsive ΔV). The two-body zero-point patched conic approximation, also referred to as the zero-sphere-of-influence patched conic approximation, is used in preliminary analysis of missions employing flyby trajectories. The method approximates the flyby as a collision of two point particles where the state of the attracting body, in this case the moon, is unaffected. In this work, V_∞ leveraging maneuvers and zero-point patched conic gravity turns are combined into resonance hopping to complete fuel and time efficient inner-moon orbital transfers.

A. Background

The delta-velocity Earth gravity assist (ΔV -EGA), the first example of a V_∞ leveraging, is introduced in (Ref. 1). Additionally, the analytic theory of two-body VILMs is developed in (Ref. 2), and it is explored further and applied to relevant problems in (Ref. 3-7). The zero-point patched conic method approximates the moon's region of influence to be infinitesimally small and the spacecraft's velocity change to be instantaneous at the point of flyby (Ref. 8). Each VILM requires the spacecraft to be in a near-resonant orbit with respect to the moon in question, so the process of moving between different near-resonant orbits from one moon to another is termed V_∞ leveraging-based resonance hopping (which is a variation of the resonance hopping technique defined in (Ref. 8)).

B. Motivation

While previous studies are focused on its heliocentric applications, it is important to note that V_∞ leveraging is not specific to the Sun-Earth system. V_∞ leveraging has considerable heritage from use in several heliocentric missions, but the associated design space in this environment is relatively small. As a result, the current state of the art of V_∞ leveraging mission design is manual point designs. Accordingly, this work studies the application of VILMs to the phase-fixed planetary moon tour problem, where the distance and time scales are dramatically different from the heliocentric problem. Various studies on different aspects of the planetary moon tour are conducted in (Ref. 8-16). In the general three-dimensional case, the region of moon influence is a sphere (Ref. 17 and 18), but in this research only the planar, circular case is considered. Tours with long flight times and very low fuel requirements using three-body applications are demonstrated in (Ref. 11, 19, and 20). On the other hand, this work is intended to be most applicable to shorter flight-time missions, such as those in the Jovian system where radiation exposure is a driving constraint.

Particular motivation for this work comes from recent interest from NASA and ESA to send flagship class tour and orbiting missions to the planetary moon system of Jupiter. In FY07, under sponsorship of NASA headquarters, the Jet Propulsion Laboratory completed the Jupiter System Observer mission study*. Concurrently, three other outer planet mission studies were completed at various research centers as part of an initiative to quickly assess potential mission scenarios for the next outer planet flagship mission. Among the many challenges facing mission design for the Jupiter System Observer and other planetary moon missions is the open issue of how to most effectively and efficiently connect the inner-moon portion of the trajectory design with the carefully selected science orbits.

In general, the end goal of this research is to design time and fuel efficient transfers between previously discovered circulating eccentric science orbits about moons in the Jovian system. Among the many options considered in the preliminary trade space for the Jupiter System Observer mission, the proposed reference mission included a one year mission phase where the spacecraft is loosely captured around Ganymede in a heavily perturbed third body orbit. The circulating orbit cycles between high and low eccentricity while distributing its close approach locations throughout most latitudes and all longitudes (Ref. 21). The orbital geometry and timing are favorable for a variety of both Ganymede and Jupiter system science. Because the dynamics of orbiters around planetary moons are largely governed by the unstable perturbing effects of the planet, the science orbit design is challenging and the resulting set of feasible orbits that satisfy mission and dynamical constraints are limited. Thus, two-body inner-moon transfers apply established V_∞ leveraging methods, basic targeting, and enumeration techniques to connect these eccentric science orbits and consequently provide one solution to the planetary moon tour problem (Ref. 22).

* http://www.lpi.usra.edu/opag/jso_final_report.pdf [cited Mar 20 2008]

II. Models

The modeling of this work is divided into three main components: V_∞ leveraging maneuver, zero-point patched-conic approximation, and resonance hopping. The following sections detail each component and discuss how these models were integrated to create the capability to find and optimize families of inner-moon transfers.

A. V_∞ Leveraging Maneuver

Phasing between the body and the spacecraft is an integral part of a VILM. At the beginning of the trajectory, the spacecraft departs from the body's orbit into a nearly resonant orbit (Ref. 2). In the case of a planetary moon system, the specific parameters of this resonance are described by the variables L (number of spacecraft orbit revolutions), K (number of moon orbit revolutions), and R_p (ratio between the spacecraft and resonant orbit periods). Additionally, M represents the spacecraft orbit revolution on which the maneuver is performed, and \pm denotes the location of the moon rendezvous (after or before the spacecraft crosses the line of apsides, respectively). This terminology is consistent with the interplanetary application of V_∞ leveraging introduced in (Ref. 2). The corresponding geometry for forward and backward interior and exterior maneuvers in the planetary moon system is depicted in Figure 1 and Figure 2.

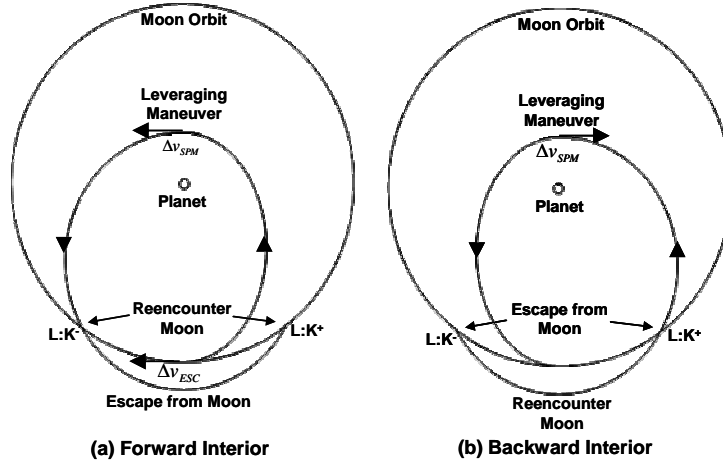


Figure 1 Interior V_∞ Leveraging Maneuver Geometry

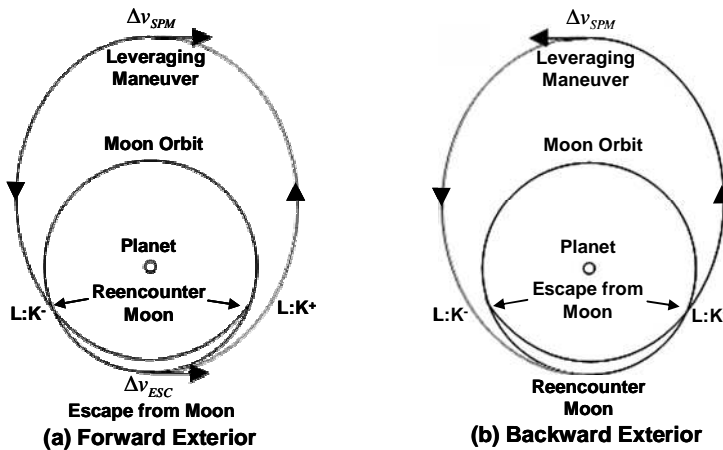


Figure 2 Exterior V_∞ Leveraging Maneuver Geometry

As can be seen in Figure 1 and Figure 2, a small propulsive burn is performed tangent to the orbit at the line of apsides crossing directly across from the launch location. In the case of a forward interior maneuver, the burn is performed in the direction of the velocity vector at the periapease of the spacecraft's orbit. The location and magnitude

of this burn allow the spacecraft to increase the size of its orbit and ultimately rendezvous with the moon at an inertial position different than that of the launch location. Alternately, a backward interior VILM reverses the effect of a forward interior maneuver so that the V_∞ magnitude decreases. A backward interior VILM departs from the \pm location that is opposite of its forward counterpart's reencounter position with its spacecraft velocity vector pointed off-tangent with respect to the moon's orbit. Furthermore, the propulsive burn at periapse occurs in the opposite direction of the spacecraft's velocity, and its rendezvous with the moon is tangent to the moon's orbit. The relative symmetry of these two maneuvers results in identical fuel usage and time of flight regardless of direction. Along these lines, Δv_{ESC} (magnitude of escape propulsive maneuver at moon) and Δv_{SPM} (magnitude of small propulsive maneuver at line of apsides) are introduced as two parameters that quantify the fuel efficiency of each VILM. Forward and backward exterior leveraging maneuvers are very similar to their interior counterparts; Figure 2 and analyses in (Ref. 1, 2, and 4) give thorough descriptions of their important similarities and differences.

This work relies on the assumption that the near-optimum location and direction of each leveraging maneuver burn is at the line of apsides and tangent to the spacecraft's orbit, respectively (Ref. 2). This standard burn location and direction could be further optimized for each maneuver, but a departure from either of these assumptions would significantly complicate the resulting flyby timing and geometry. In fact, it is well known that changing the V_∞ is akin to changing the Jacobi constant in the three-body problem (Ref. 4 and 20). Further, the maximum change in Jacobi constant occurs when a maneuver is performed tangent to the orbit and at the apsides where the rotating velocity is greatest (Ref. 4). Therefore, the stated burn location and direction are indeed optimal for maximizing the change in V_∞ during a single leveraging maneuver.

The current work also assumes that the spacecraft always escapes from and returns to the moon tangent to both orbits during forward and backward VILMs, respectively. Again, this key starting or ending direction could be marginally improved when optimizing multiple sequences of maneuvers, but as already discussed, V_∞ is most efficiently changed when the rotating velocity is greatest. The tangent departure provides for the maximum (or minimum) apse distance, thereby optimizing the potential for change in V_∞ . Furthermore and perhaps more importantly, applying the tangential strategy allows the local problem to be decoupled from the global pathfinding problem.

B. Zero-Point Patched-Conic Approximation

In order to complete each step of the resonance hopping procedure, a specific change in V_∞ is targeted for each VILM; the targeted change in V_∞ is necessary for the spacecraft to achieve its next near-resonant orbit in the path. The V_∞ change that results from a single VILM is controlled by varying three of its defining parameters. Specifically, the three influential parameters in question are R_p (continuous), M (discrete), and \pm (discrete). For a given set of M and \pm values, the problem is reduced to a simple one-dimensional root-solving problem to identify the R_p that leads to the targeted change in V_∞ (as the physical dynamics allow). Upon arriving at the moon with the correct V_∞ , a zero-point patched conic flyby is completed at rendezvous to turn the spacecraft's velocity back to (or away from) tangent with the moon's orbit so the VILM process can be repeated. Figure 3 is a visual representation of the planet-relative and moon-relative velocities during the flyby.

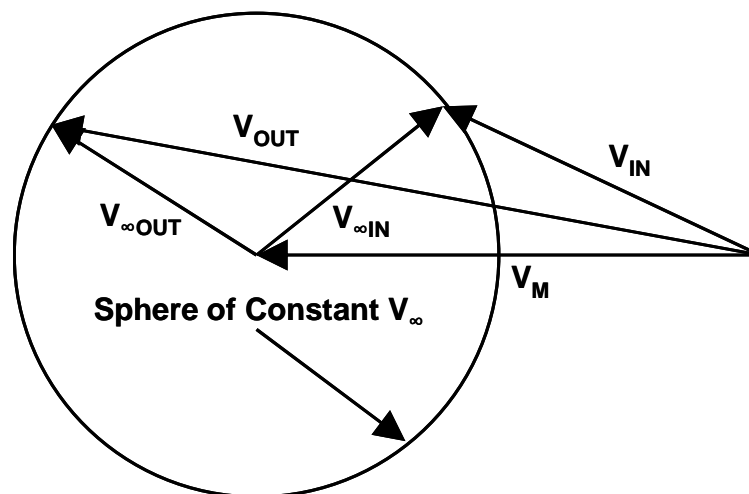


Figure 3 Two-Body Zero-Point Patched Conic Velocity Diagram

In Figure 3, \mathbf{V}_{IN} and \mathbf{V}_{OUT} are the planet-relative spacecraft approach and departure velocity vectors, and \mathbf{V}_M is the velocity vector of the moon with respect to the planet. The zero-point patched conic model implies that the incoming and outgoing hyperbolic excess velocities have the same magnitude (Ref. 23). It is well known that this model is a better approximation in the interplanetary problem than the planetary moon problem. However, the approximation does remain useful and is successfully employed in preliminary design for many complex planetary moon tours (Ref. 12 and 24).

C. Resonance Hopping

While transfers between two moons are symmetric regardless of direction, this work focuses on the design of interior inner-moon transfers because they are more likely to be included in realistic moon tour missions. The procedure to accomplish this task is broken into the two phases depicted in Figure 4.

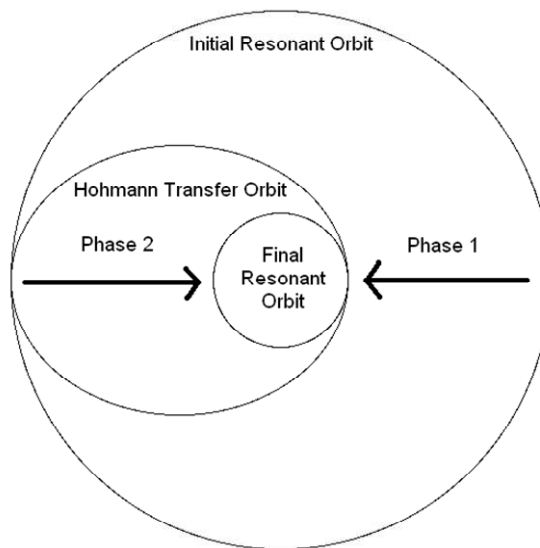


Figure 4 Interior Inner-moon Transfer Phase Diagram

As can be seen in Figure 4, Phase 1 of the transfer involves changing the spacecraft V_∞ from the initial resonant orbit V_∞ to the Hohmann transfer (HT) V_∞ between the two moon orbits. The necessary V_∞ change for Phase 1 is accomplished using a resonance hopping procedure comprised of alternating forward interior VILMs (see Figure 2) and zero-point patched conic flybys. Phase 1 finishes when the spacecraft passes near the arrival moon tangentially after it completes the inner-moon HT. Phase 2 of the transfer involves changing from the inner-moon HT periapse V_∞ to the final resonance orbit V_∞ . Similar to Phase 1, this V_∞ change is accomplished using alternating flybys and VILMs, but this time the flybys turn the spacecraft velocity vector away from tangent and the maneuvers are of the backward exterior variety (see Figure 2). Phase 2 begins with a gravity turn at the initial arrival moon rendezvous point, which provides the necessary initial velocity vector orientation for the first backward exterior VILM. Phase 2 finishes when the spacecraft re-encounters the arrival moon with a V_∞ that corresponds to the final resonant orbit. The initial relative phase angle between the two moons (θ) represents the relative initial geometry that is required to ensure that the arrival moon is in the correct position upon completion of the phase patching HT.

IV. Methodology

A multi-level procedure is used to calculate and analyze the solutions to each inner-moon V_∞ leveraging transfer problem. The objective is to patch a known sequence of near-resonant orbits with gravity assisted flybys. VILMs are designed to progressively adjust the V_∞ at each flyby to the level appropriate for the subsequent resonant orbit. The V_∞ for a given L:K resonance is easily calculated using the expression in Eq. (1).

$$V_\infty = \frac{V_M(L-K)}{K} \quad (1)$$

Once the resonant V_∞ is calculated, a value slightly above or below (depending on the particular VILM geometry) this reference is targeted so the spacecraft enters into the appropriate near-resonant orbit. The inner-level algorithm calculates the characteristics of the VILM trajectory and subsequently root-solves for VILMs that result in the targeted change in V_∞ . The algorithm adjusts the magnitude of the small propulsive burn (Δv_{SPM}) to ensure that a spacecraft-moon rendezvous occurs at the intended \pm orbit intersection (Ref. 2). Then, for each combination of the discrete variables M and \pm , the continuous R_p value is adjusted until the targeted change in V_∞ is achieved (as the physical dynamics allow). Since flybys are such an integral part of the resonance hopping procedure, maneuvers with unrealistic approach radii are filtered out and not considered further. The accepted expression for necessary radius of closest approach ($r_{P_{nec}}$) is shown in Eq. (2).

$$r_{P_{nec}} = \frac{\mu_m}{V_\infty^2 \sin(k_{nec}/2)} - \frac{\mu_m}{V_\infty^2} \quad (2)$$

The necessary flyby radius must be greater than the mission's specified minimum radius of closest approach ($r_{P_{min}}$) in order for the corresponding VILM to be considered viable. Once all of the targeted maneuvers are enumerated and filtered, the inner-level algorithm returns the single VILM that achieves the targeted V_∞ change in the most fuel efficient manner.

The outer-level algorithm calculates and analyzes all of the possible resonance combinations, or hopping paths, between the two transfer moons. An exhaustive list of all of the possible L:K resonant orbits is created based on the initial and final resonances as well as maximum allowable time of flights for each phase. Table 1 shows a list of possible resonant orbits for Phase 1 of a Ganymede to Europa transfer with a 6:5 initial resonance and a three-month maximum allowable time of flight.

Table 1 Possible Resonant Orbits for Phase 1 of Ganymede-Europa Transfer

L	K	L/K
Initial V_∞ (6:5)		1.2000
5	4	1.2500
9	7	1.2857
4	3	1.3333
8	6	1.3333
Hohmann Transfer (HT)		1.3632

Although Table 1 includes only four potential resonances, it is important to note that a maximum flight time of a six months leads to 32 potential resonances to consider. While repeat L:K ratios (i.e. 4:3 and 8:6) are allowed at this stage due to the potential to vary the maneuver revolution, the results will show that the shorter flight time solutions are almost always preferable. Based on the list of possible resonances, a resonance hopping tree is then created to enumerate all of the useful combinations, or hopping paths, of the resonant orbits that are within the allowable time of flight. This tree configuration is created by starting at the HT orbit and working backwards through each resonant path until the given initial resonance orbit is reached, a backward sweep technique based on the principles of Bellman's Dynamic Programming (Ref. 25). Figure 5 shows the resonance hopping tree that is created from Table 1's data, along with its corresponding numbering system.

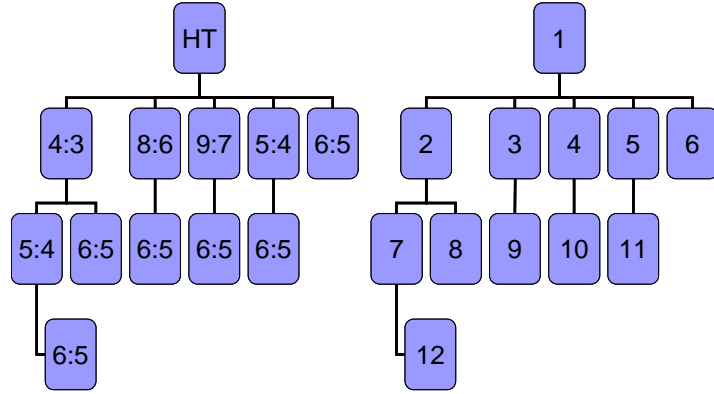


Figure 5 Resonance Hopping Tree for Phase 1 of Ganymede-Europa Transfer

Each branch of the example resonant tree starts at a 6:5 box and terminates at the HT box; consequently, each branch represents a complete resonance hopping path. All of the possible resonant paths are reconstructed by organizing the tree's boxes in a matrix. Each resonant box is given an ascending integer from left to right down each row, or generation. Then, each box's parent (the connecting box from the previous generation) and current total moon revolutions (the sum of K from the L:K terminology) are collected and organized in matrix form. A tree enumeration matrix created from the tree in Figure 5 is shown in Table 2.

Table 2 Tree Enumeration Matrix for Phase 1 of Ganymede-Europa Transfer

Current Box #	Parent Box #	L	K	L/K	Total K
1	-	-	-	1.3632	-
2	1	8	6	1.3333	6
3	1	4	3	1.3333	3
4	1	9	7	1.2857	7
5	1	5	4	1.2500	4
6	1	6	5	1.2000	5
7	2	6	5	1.2000	11
8	3	5	4	1.2500	7
9	3	6	5	1.2000	8
10	4	6	5	1.2000	12
11	5	6	5	1.2000	9
12	8	6	5	1.2000	12

After the data points are collected and organized in the tree enumeration matrix, each path is reconstructed by starting at each row with the initial resonance and following the parent trail up to the HT (Box #1). Table 3 illustrates the reconstruction from bottom to top of one path from the matrix.

Table 3 Example Resonant Path Reconstruction for Ganymede-Europa Phase 1 Transfer

Current Box #	Parent Box #	L/K
12	8	1.2000
8	3	1.2500
3	1	1.3333

Once all of the resonant paths for each transfer phase have been reconstructed, the inner-level algorithm described at the beginning of this section is used to target and optimize the set of VILMs that are necessary to change the spacecraft V_{∞} from the specified initial to final resonance. The resulting complete trajectory total ΔV and time of flight for each path is then organized in the form of a scatter plot which represents the fuel versus flight time trade study that is critical for preliminary design.

V. Results

The aforementioned procedure is used to generate fuel versus flight time trade study results for a variety of transfers between several moons in the Jovian system. All of these moon orbits are approximated as circular and coplanar, and their orbit radii, body radii, and gravitational parameters are listed in Table 4*.

Table 4 Jovian System Moon Orbit and Physical Characteristics

Moon	Orbit Radii (km)	Body Radii (km)	Gravitational Parameter (km ³ /s ²)
Callisto	1882700	2410.3	7.1795e3
Ganymede	1070400	2631.2	9.8879e3
Europa	671100	1560.8	3.2027e3
Io	421800	1821.6	5.959e3

All of the possible V_∞ leveraging-based resonance hopping paths between the four representative moons are calculated and analyzed based on several realistic numerical assumptions. Minimum flyby altitude is set at 100 km, and the maximum allowable time of flight for each transfer is set at 20 times the orbital period of the departure moon. The initial and final resonances, 6:5 and 5:6, respectively, are chosen to be consistent with realistic flight time constraints and low energy tours (Ref. 11 and 26). If the VILM sequences are initiated or terminated with low altitude orbit insertion at one of the moons, (Ref. 26) gives a simple quadrature for the optimal boundary V_∞ conditions. On the other hand, the transfers in this work begin and end with near-resonant orbits around the central body. In other words, the orbit insertion costs that are left out of this analysis cover the aforementioned escape propulsive maneuver for each transfer, so total fuel costs for the following trajectories are based on the sum of their small propulsive maneuvers. The resulting scatter plot of possible trajectories between Ganymede and Europa is shown in Figure 6, where the numbered trajectories comprise the Pareto front; scatter plots for the remaining Jovian system inner-moon transfers can be found in (Ref. 22).

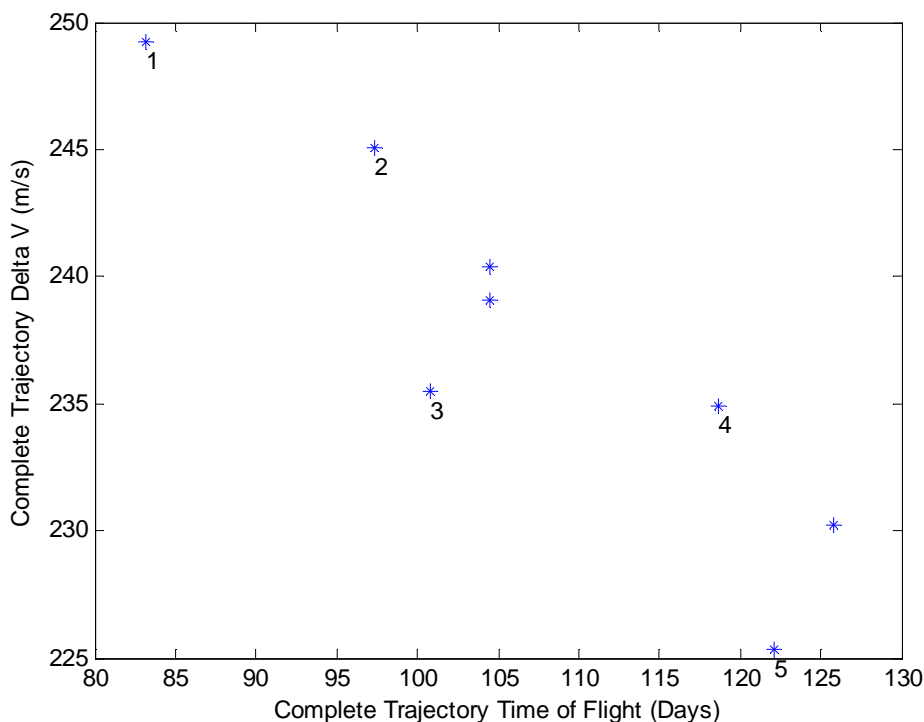


Figure 6 Complete Trajectory Scatter Plot for Ganymede-Europa (6:5-5:6) Transfer

Each point in Figure 6 represents a complete resonant hopping sequence, or branch of the previously depicted tree (see Figure 5). Table 5 shows a comparison of each transfer's fuel and time optimum trajectories (FOT and

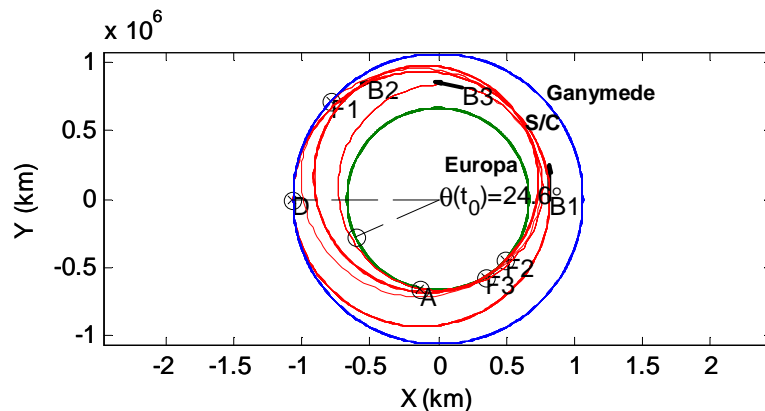
* URL: <http://ssd.jpl.nasa.gov/> [cited 16 Jan 2009].

TOT, respectively) from the aforementioned scatter plots. The maximum allowable times of flight and transfer distances are normalized by the orbit period and radii of the departure moon, respectively.

Table 5 Jovian System Time and Fuel Optimum Trajectory Costs

Transfer Moons (Departure- Arrival)	Transfer Distance/ Departure Moon Radii	TOT ΔV (m/s)	TOT Flight Time (days)	FOT ΔV (m/s)	FOT Flight Time (days)	Max. TOF/ Departure Moon Period
Callisto- Ganymede	0.4314	289.3	156.9	279.6	214.0	20
Ganymede- Europa	0.3734	249.2	83.14	225.3	122.1	20
Europa-Io	0.3715	259.0	50.20	254.7	62.55	20

As can be seen in Table 5, the difference in ΔV cost between the Callisto-Ganymede FOT and TOT is very small (~3%, which is consistent with the phase free results from (Ref. 26)), but the difference in time of flight is quite large (~27%). Similar trends occur in the data from the other two Jovian system inner-moon transfers. As a result, the TOT of each transfer is chosen for further consideration because it is consistently the most efficient option in this design space. The orbital trajectory diagram seen in Figure 7 depicts the motion of the three bodies during the Ganymede to Europa transfer's TOT; orbital trajectory diagrams for the remaining Jovian system inner-moon transfer TOTs can be found in (Ref. 22).



Event #	Time (days)	Event
1	0	D (6:5, $ V_\infty = 0.7288$ km/s)
2	32.78	B1 ($\Delta V = 127.2$ m/s)
3	34.94	F1 (HT, $ V_\infty = 1.329$ km/s, $r_{nec} = 5330$ km)
4	37.56	F2 (5:7, $ V_\infty = 1.494$ km/s, $r_{nec} = 3992$ km)
5	44.84	B2 ($\Delta V = 22.99$ m/s)
6	62.25	F3 (5:6, $ V_\infty = 1.320$ km/s, $r_{nec} = 1789$ km)
7	63.96	B3 ($\Delta V = 99.04$ m/s)
8	83.14	A (5:6, $ V_\infty = 0.7665$ km/s)

Figure 7 Complete Orbital Trajectory Diagram for Ganymede-Europa (6:5-5:6) Transfer TOT

In Figure 7, departure (D), burn (B), flyby (F), and arrival (A) times and locations are all labeled, and the initial phasing angle (θ) between the two transfer moons is depicted.

Figure 6, Figure 8, and Table 6 show the results of repeating the earlier Ganymede to Europa transfer analysis with a 50% longer allowable maximum time of flight and comparing their respective fuel optimum trajectories (FOT); the additional Jovian system Table 6 data is collected from similar scatters plots found in (Ref. 22).

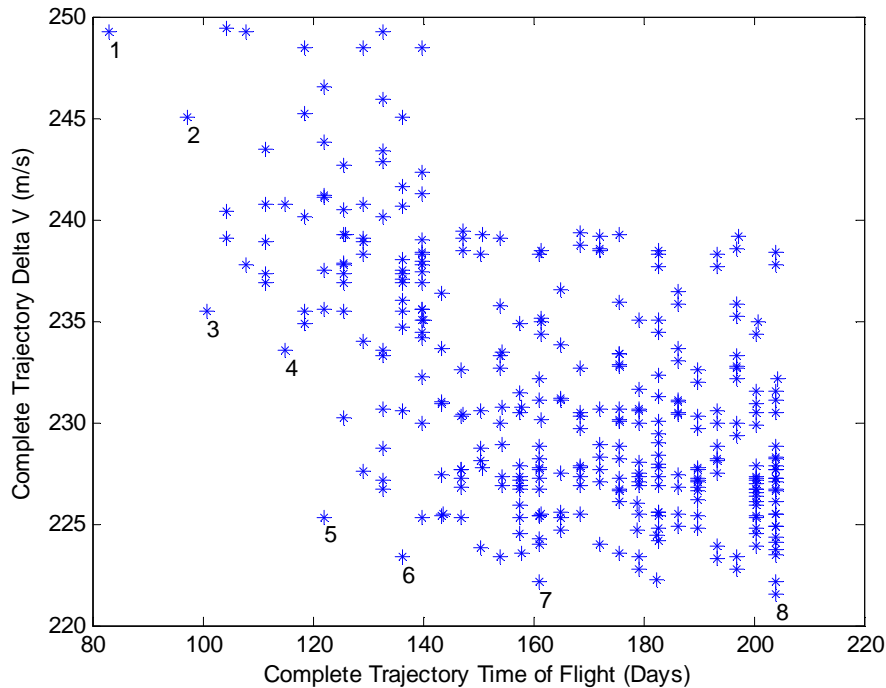


Figure 8 Complete Trajectory Scatter Plot for Long TOF Ganymede-Europa (6:5-5:6) Transfer

Table 6 Jovian System Maximum Allowable Time of Flight Experiment Results

Transfer Moons (Departure-Arrival)	FOT ΔV (m/s)	FOT Flight Time (days)	Max. TOF/ Departure Moon Period	FOT ΔV (m/s)	FOT Flight Time (days)	Max. TOF/ Departure Moon Period
Callisto- Ganymede	279.6	214.0	20	249.1	454.0	30
Ganymede- Europa	225.3	122.1	20	221.5	204.0	30
Europa-Io	254.7	62.55	20	245.7	89.01	30

It is known from phase-free theory that a mathematical limit for the minimum ΔV for leveraging transfers between moons exists (Ref. 26), and the data from Table 6 substantiates this claim. In other words, increasing the maximum allowable time of flight by 50% only marginally improves the fuel cost and significantly increases the trajectory time of flight. Along these lines, (Ref. 26) gives a quadrature expression for the theoretical minimum fuel limit for exterior and interior leveraging. Unlike the theoretical explanation, the results of this study not only clearly indicate the existence of the aforementioned limit, but they also indicate the approximate time of flight where the Pareto front approaches it.

Finally, full planetary moon tour costs are calculated by adding the TOT fuel and flight time totals for multiple transfers in the same system. Table 7 shows the fuel and time of flight costs for a full planetary moon tour from Callisto to Io with intermediate loosely captured orbits at Ganymede and Europa to gather scientific information.

Table 7 Jovian System Moon Tour Costs

Transfer Moons (Departure-Arrival)	TOT Total ΔV (m/s)	TOT Time of Flight (days)
Callisto-Ganymede	289.3	156.9
Ganymede-Europa	249.2	83.14
Europa-Io	259.0	50.20
Complete Tour	797.5	290.24

These loosely captured science orbits don't require any additional propulsive burns; alternatively, it is estimated that insertion and departure from low altitude science orbits would cost less than 100 m/s per moon. A similar tour analysis was considered for the Saturnian system, but the unique physical characteristics and dynamics of its moons make it very difficult for this particular procedure to complete transfers involving them. It is important to note that completing each of these tours in the reverse direction would involve identical fuel and time of flight costs due to the leveraging maneuvers' inherent symmetry. Also, additional time and fuel would need to be allotted for a actual mission to account for science and phasing as well as orbit departure and insertion considerations.

VI. Conclusions

The resonance hopping and associated pathfinding technique developed in this study addresses the phase-fixed planetary moon tour problem. This research offers an automated alternative that efficiently produces families of Pareto optimized trajectory solutions, which is necessary due to the considerable size of the planetary moon tour design space. A preliminary design software tool in MATLAB has been written that utilizes the aforementioned procedure to solve the phasing and resonant pathfinding problem associated with planetary moon tours. Additionally, applying V_∞ leveraging in the heliocentric environment requires a system design trade involving launch energy versus mid-course correction fuel and tank considerations. The planetary moon tour problem does not require this trade, which makes V_∞ leveraging a more viable mission design option in this environment from a systems engineering perspective. Furthermore, this approach verifies fuel costs predicted by phase free theory, and it provides the flight times associated with these fuel limits that are inherently missing from theory. Along these lines, lower fuel tour solutions are possible using multi-body models, but these trajectories typically involve long flight times (Ref. 20). Therefore, the results from this work are most useful for missions requiring short flight times, which is a likely constraint for future planetary moon tour missions. Finally, it is important to note that the zero-point patched conic moon tour solutions from this research should be used as preliminary designs that give useful initial estimations and ultimately lead to the discovery of more robust trajectories from three-body and ephemeris models.

VII. Acknowledgements

The author thanks Ryan Russell first and foremost for serving as the sole advisor for the entirety of this research and co-author for the journal and conference papers that were by-products of this work. The author also thanks Jechiel Jagoda, Robert Braun, Cynthia Pendley, Christopher Marsh, Anastassios Petropoulos, Jon Sims, and Nathan Strange for their interest and support of this research. This work was carried out at the Georgia Institute of Technology's Space Systems Design Laboratory, with partial support from the Jet Propulsion Laboratory.

References

- ¹ G. R. Hollenbeck, "New Flight Techniques for Outer Planet Missions," AAS Paper 75-087.
- ² J. A. Sims, J. M. Longuski, and A. J. Staugler, " V_{∞} Leveraging for Interplanetary Missions: Multiple-Revolution Orbit Techniques," *Journal of Guidance, Control, and Dynamics*, Vol. 20, No. 3, 1997, pp. 409-415.
- ³ N. A. Strange and J. A. Sims, "Methods for the Design of V-Infinity Leveraging Maneuvers," AAS Paper 01-437.
- ⁴ T. H. Sweetser, "Jacobi's Integral and ΔV -Earth-Gravity-Assist (ΔV -EGA) Trajectories," AAS Paper 93-635.
- ⁵ L. Casalino, G. Colasurdo, and D. Pastrone, "Optimization of ΔV -Earth-Gravity-Assist Trajectories," AAS Paper 97-713.
- ⁶ N. J. Strange and J. M. Longuski, "Graphical Method for Gravity-Assist Trajectory Design," *Journal of Spacecraft and Rockets*, Vol. 39, No. 1, 2002, pp. 9-15.
- ⁷ J. A. Sims, A. J. Staugler, and J. M. Longuski, "Trajectory Options to Pluto Via Gravity Assists from Venus, Mars, and Jupiter," *Journal of Spacecraft and Rockets*, Vol. 34, No. 3, 1997, pp. 347-353.
- ⁸ C. Uphoff, P. H. Roberts, and L. D. Friedman, "Orbit Design Concepts for Jupiter Orbiter Missions," *Journal of Spacecraft and Rockets*, Vol. 13, No. 6, 1976, pp. 348-355.
- ⁹ A. A. Wolf and J. C. Smith, "Design of the Cassini Tour Trajectory in the Saturnian System," *Control Eng. Practice*, Vol. 3, No. 11, 1995, pp. 1611-1619.
- ¹⁰ J. C. Smith, "Description of Three Candidate Cassini Satellite Tours," AAS Paper 98-106.
- ¹¹ S. D. Ross, W. S. Koon, M. W. Lo, and J. E. Marsden, "Design of a Multi-Moon Orbiter," AAS Paper 03-143.
- ¹² A. F. Heaton, N. J. Strange, J. M., Longuski, and E. P. Bonfiglio, "Automated Design of the Europa Orbiter Tour," *Journal of Spacecraft and Rockets*, Vol. 39, No. 1, 2002, pp. 17-21.
- ¹³ G. J. Whiffen, "An Investigation of a Jupiter Galilean Moon Orbiter Trajectory," AAS Paper 03-544.
- ¹⁴ A. F. Heaton and J. M. Longuski, "Feasibility of a Galileo-Style Tour of the Uranian Satellites," *Journal of Spacecraft and Rockets*, Vol. 40, No. 4, 2003, pp. 591-595.
- ¹⁵ N. J. Strange, T. D. Goodson, and Y. Hahn, "Cassini Tour Redesign for the Huygens Mission," AIAA Paper 2002-4720.
- ¹⁶ L. Casalino, G. Colasurdo, and M. R. Sentinella, "Low-Thrust Trajectories to Mercury with Multiple Gravity Assists," AIAA Paper 2007-5233.
- ¹⁷ R. P. Russell and C. A. Ocampo, "Geometric Analysis of Free-Return Trajectories Following a Gravity-Assisted Flyby," *Journal of Spacecraft and Rockets*, Vol. 42, No. 1, 2005, pp. 694-698.
- ¹⁸ N. J. Strange, R. P. Russell, and B. Buffington, "Mapping the V-Infinity Globe," AAS Paper 07-277.
- ¹⁹ S. D. Ross and D. J. Scheeres, "Multiple Gravity Assists in the Restricted Three-Body Problem," AAS Paper 07-227.
- ²⁰ S. Campagnola and R. P. Russell, "The Endgame Problem PART B: The Multi-Body Technique and the TP Graph," AAS Paper 09-227.
- ²¹ R. P. Russell and A. T. Brinckerhoff, "Circulating Eccentric Orbits Around Planetary Moons," *Journal of Guidance, Control, and Dynamics*, Volume 32, No. 2, 2009, pp. 424-436.
- ²² A. T. Brinckerhoff and R. P. Russell, "Pathfinding and V-Infinity Leveraging for Planetary Moon Tour Missions," AAS Paper 09-222.
- ²³ C. Uphoff and M. A. Crouch, "Lunar Cyclor Orbits with Alternating Semi-Monthly Transfer Windows," AAS Paper 91-105.
- ²⁴ R. P. Russell and N. J. Strange, "Planetary Moon Cyclor Trajectories," *Journal of Guidance, Control, and Dynamics*, Vol. 32, No. 1, 2009, pp. 143-157.
- ²⁵ R. Bellman and S. E. Dreyfus, *Applied Dynamic Programming*, Princeton University Press, Princeton, NJ, 1962.
- ²⁶ S. Campagnola and R. P. Russell, "The Endgame Problem PART A: V-infinity Leveraging Technique and the Leveraging Graph," AAS Paper 09-224.